Reducing the linewidth of hybrid integrated III-V/silicon laser by utilizing high-Q multimode-waveguide-based silicon ring resonator

Xinhang Li[1], Yuyao Guo[1,2,*], Siyu E[1], Yihao Fan[1], Minhui Jin[1,2], Weihan Xu[1], Liangjun Lu[1,2], Yu Li[1,2], Jianping Chen[1,2], and Linjie Zhou[1,2]

[1]State Key Laboratory of Advanced Optical Communication Systems and Networks, Shanghai Key Lab of Navigation and Location Services, Department of Electronic Engineering, Shanghai Jiao Tong University, Shanghai 200240, China
[2]SJTU-Pinghu Institute of Intelligent Optoelectronics, Pinghu, 314200, China
**Author e-mail address: guoyuyao1992@sjtu.edu.cn*

Abstract: We demonstrate a hybrid integrated self-injection locking laser (SIL) with an intrinsic linewidth of 1.25 kHz and an external cavity laser (ECL) of 5.3 kHz by leveraging a high-Q multimode-waveguide-based silicon microring resonator (MRR).

1. Introduction

Narrow-linewidth semiconductor lasers find extensive application in various fields that demand high spectral purity and low noise, including optical fiber communication, quantum information processing, and light detection and ranging (LiDAR) [1, 2], etc. The hybrid integrated lasers, particularly the SIL and ECL designs, present a promising solution for achieving narrow linewidth by combining a III-V chip with a low-loss passive optical cavity. Silicon nitride (Si_3N_4) platform is often used to make the external optical cavity due to its low loss. However, its footprint is relatively large due to the small refractive index contrast of the Si_3N_4 waveguide. Moreover, phase tuning of Si_3N_4 is mainly based on the thermo-optic effect, which limits the tuning speed to tens of kilohertz [3]. The silicon-on-insulator (SOI) platform has the merits of compact footprint, low cost, low power consumption, and high tuning speed (hundreds of kilohertz). However, high linear and nonlinear loss of the silicon waveguides from side wall roughness and two-photon absorption (TPA) limit the intrinsic linewidth of III-V/Si hybrid integrated lasers to 10's~100's kilohertz. Benefiting from the large waveguide mode, the linewidth has been reduced to hundreds of hertz level on the thicker silicon (400 nm~500 nm) waveguide platform [4], but it is hard to integrate many mature silicon active devices for large-scale photonic integrated circuits. In the frequently employed 220-nm-thick SOI platform, multimode waveguides are commonly utilized to attain low-loss waveguides and high-Q microring resonators (MRR) with minimal overlap between the optical mode and sidewall [5]. Moreover, the expanded optical mode area in multimode waveguides results in a reduced power density, thereby mitigating the impact of TPA. Consequently, employing a multimode-waveguide-based high-Q MRR in a III-V/silicon laser holds promise for achieving a narrow linewidth.

In this work, we present III-V/silicon hybrid SIL and ECL with multimode-waveguide-based high-Q MRR fabricated on the 220-nm SOI platform. Leveraging the MRR's advantageous characteristics, such as low loss, large effective volume, and high power handling capability, we measured an intrinsic linewidth of 1.25 kHz for the SIL (202 times narrower than the free-running state) and 5.3 kHz for the ECL.

2. Design and structure

Figure 1(a) shows the schematic structure of the multimode-waveguide-based high-Q MRR. A portion of the MRR is replaced by two straight multimode ridge waveguides. As shown in Fig. 1(b), the thickness and width of the silicon multimode waveguide are 220 nm and 2 μm, and the height of the slab is 90 nm. It can be seen from the optical mode profile in the inset of Fig. 1(a), that the optical mode is tightly confined in the multimode waveguide and the overlap between the optical mode and the sidewall is greatly reduced. The measured multimode waveguide propagation loss is about 0.1 dB/cm near 1550 nm. Four linear tapers with a length of 100 μm are utilized to ensure the adiabatic transformation of TE_0 mode from the multimode ridge waveguide to the single-mode ridge waveguide of 0.5 μm wide. The bending radius of the single-mode waveguide is 20 μm. The gap between the bus waveguide and the MRR is set to be 230 nm and the simulated power coupling coefficient is 0.15. To characterize the silicon high-Q MRR, we measured the transmission spectra with a commercial tunable laser (Keysight 8164A). The transmission spectra of the MRR used in the SIL are depicted in Fig. 1(c). The FSR near 1550 nm is about 0.155 nm. Figure 1(d) is the enlarged view of the transmission spectrum near 1549.14 nm. A Lorentz-type function (orange line) is utilized to fit the measured data (blue dots). The full width at half maximum (FWHM) is about 8 pm and the loaded-Q factor is 1.9×10^5.

Figures 1(e) and (f) are the schematic structures of the proposed SIL and ECL, respectively. For the SIL, a commercially available distributed feedback (DFB) laser is butt-coupled to the high-Q MRR silicon chip. An inverse taper on the passive circuit is used to reduce the coupling loss between chips. The length of straight multimode ridge waveguides of the high-Q MRR is 1815 µm. The ECL consists of an InP reflective semiconductor optical amplifier (RSOA) butt-coupled to an external silicon photonic chip. The external chip incorporates a Vernier filter composed of three MRRs. MRR_1 and MRR_2 are made of single-mode ridge waveguides with slightly different circumferences of 323 µm and 336 µm, respectively. MRR_3, similar to the MRR employed in the SIL, is constructed using a multimode waveguide. However, MRR_3 has a shorter multimode waveguide length of 1200 µm. The FSRs of the three MRRs are calculated to be 1.91 nm, 1.84 nm, and 0.219 nm. The filter based on the three cascaded MRRs allows single longitudinal mode lasing when the resonance peaks of the three sets of transmission spectra are precisely aligned. Therefore, the ECL can support a wide wavelength tuning range with an extended FSR of about 50 nm. The other structures are similar with our previous work [6]. The footprint of the SIL and ECL chips are 0.2 mm × 3 mm and 0.35 mm × 3 mm, respectively.

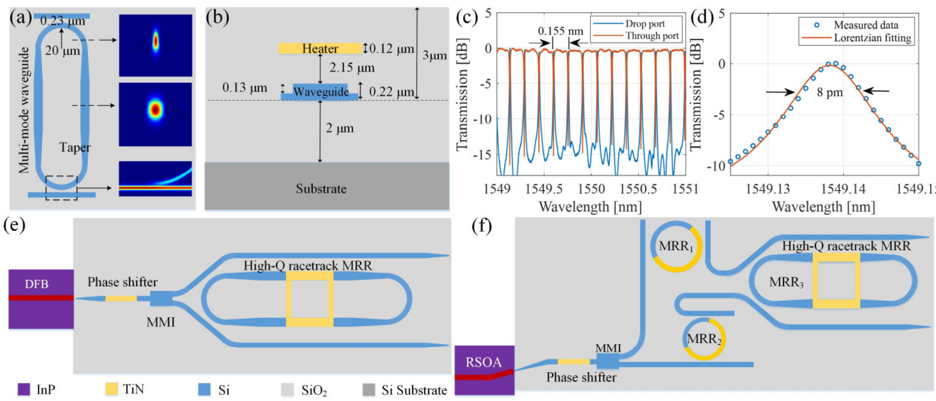

Fig. 1. (a) Left: structure of the high-Q MRR. Right: electric field intensity distribution of the single-mode waveguide, the multi-mode waveguide, and the coupler (from up to bottom). (b) Cross section of the silicon ridge waveguide tuned by a TiN micro-heater. (c) Measured transmission spectrum of the through port (orange) and drop port (blue) of the MRR. (d) Enlarged view of the resonant peak near 1549.14 nm. (e, f) Schematic structures of the SIL (e) and the ECL (f).

3. Laser performance characterization

For the SIL, the DFB laser wavelength is around 1547 nm. A self-injection locked single-mode state can be attained by thermally adjusting one resonance of the MRR to align with the longitudinal mode of the DFB laser. This alignment is facilitated by the small FSR and the high thermal tuning efficiency of approximately 4.6 pm/mW. Figure 2(a) shows the measured L-I-V curves of the laser. The maximum on-chip output power is about 4.26 mW at a pump current of 164 mA. An optical spectrum analyzer (OSA, YOKOGAWA, AQ6370D-12) with a resolution of 0.02 nm is used to measure the lasing spectrum. As shown in Fig. 2(b), the SMSR is larger than 55 dB. Figure 2(c) shows the measured optical frequency noise of the SIL. By multiplying the white noise level in the high-frequency end by π, we obtain the intrinsic linewidths of 254 kHz and 1.25 kHz at the free-running and injection-locked states, respectively. The linewidth is reduced by 202 times under the injection-locked state compared to the free-running, due to optical feedback from the high-Q silicon MRR.

For the ECL, laser wavelength tuning is achieved by adjusting the MRRs and the phase shifter. We measured the L-I-V curve of the ECL at the 1583 nm wavelength, as shown in Fig. 3(a). The maximum on-chip output power is 5

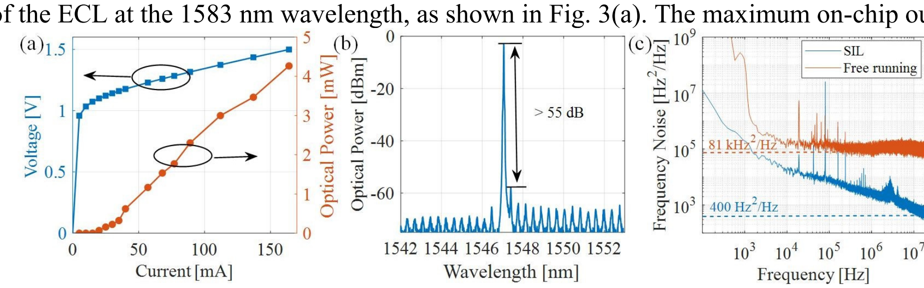

Fig. 2. (a) L-I-V curves of the SIL. (b) Single lasing spectrum under the pump current of 164 mA. (c) Frequency noise spectra measured at the free-running state (orange) and the self-injection locking state (blue).

mW under the pump current of 200 mA. The output power can be further increased by raising the pump current and improving the coupling efficiency between the RSOA and the external chip. Figure 3(d) is the superimposed lasing spectra of the ECL. The tuning range is more than 54 nm with the SMSR being more than 43 dB. The maximum SMSR is about 50.5 dB at the 1587 nm wavelength as shown in Fig. 3(b). As shown in Fig. 3(c), the minimum intrinsic linewidth of the ECL is measured to be 5.34 kHz at the 1583 nm wavelength.

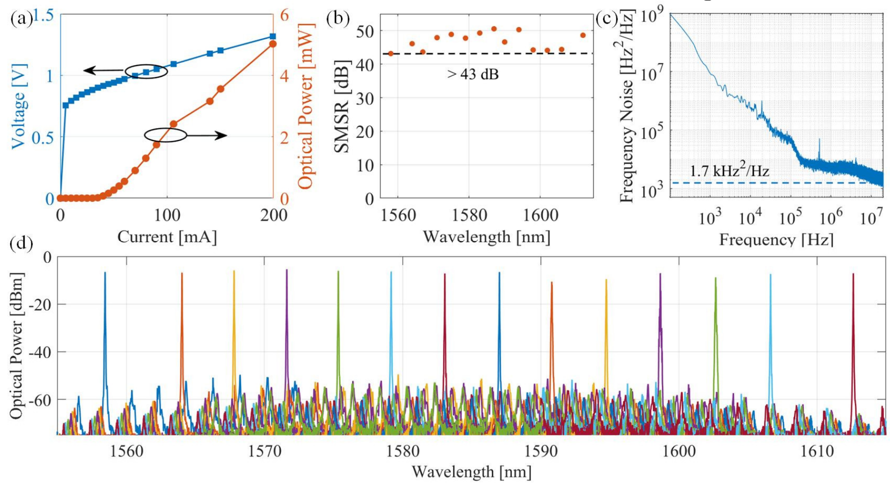

Fig. 3. (a) L-I-V curves of the ECL. (b) Extracted SMSR over the full wavelength tuning range. (c) Frequency noise spectrum at the 1583 nm wavelength. (d) Superimposed lasing spectra of the ECL.

Table 1 presents a performance comparison of hybrid lasers. As far as our knowledge extends, our SIL represents the first hybrid integrated SIL on the 220 nm silicon photonics platform. Additionally, both our SIL and ECL exhibit the narrowest intrinsic linewidth compared to previous reports on hybrid cavity lasers implemented on the 220 nm silicon platform within the C band.

Table 1. Performance comparison of hybrid integrated lasers on the 220 nm silicon platform

Year	Structure	Output (mW)	Tuning range (nm)	SMSR (dB)	Linewidth (kHz)
2018 [7]	2-MRR ECL	11	60	>46	37
2021 [8]	2-MRR ECL	>2	50	>40	105
2022 [9]	Lattice filter+MRR	>2	32	>40	27
2023 [10]	2-MRR ECL	76	70	>50	12
This	SIL	4.26	--	55	1.25
work	3-MRR ECL	5	54	>43	5.3

4. Conclusion

We have implemented two narrow-linewidth III-V/silicon hybrid lasers utilizing the multimode-waveguide-based high-Q MRRs. The SIL and ECL exhibit a narrow linewidth of 1.25 kHz and 5.3 kHz, respectively. These lasers have potential applications in optical coherent communications, LiDARs, and fiber sensors.

References

1. W. Xu, et al., "Fully integrated solid-state LiDAR transmitter on a multi-layer silicon-nitride-on-silicon photonic platform," J. Lightwave Technol. **41**, 832-840 (2023).
2. L. Li, et al., "Continuous-variable quantum key distribution with on-chip light sources," Photon. Res. **11**, 504-516 (2023).
3. Y. Guo, et al., "Thermally tuned high-performance III-V/Si_3N_4 external cavity laser," IEEE Photon. J. **13**, Art. no.1500813 (2021).
4. P. A. Morton, et al., "Integrated coherent tunable laser (ICTL) with ultra-wideband wavelength tuning and sub-100 Hz Lorentzian linewidth," J. Lightwave Technol. **40**, 1802-1809 (2022).
5. Y. Zhang, et al., "Design and demonstration of ultra-high-Q silicon microring resonator based on a multi-mode ridge waveguide," Opt. Lett. **43**, 1586-1589 (2018).
6. Y. Guo, et al., "III-V/Si hybrid external-cavity laser utilizing TM mode in the passive photonic circuit," in *OptoElectronics and Communications Conference (OECC)* (IEEE, 2022), paper TuD2-6.
7. H. Guan, et al., "Widely-tunable, narrow-linewidth III-V/silicon hybrid external-cavity laser for coherent communication," Opt. Express **26**, 7920-7933 (2018).
8. Y. Xu, et al., "Hybrid external-cavity lasers (ECL) using photonic wire bonds as coupling elements," Sci. Rep. **11**, 1-10 (2021).
9. T. Aihara, et al., "Heterogeneously integrated widely tunable laser using lattice filter and ring resonator on Si photonics platform," Opt. Express **30**, 15820-15829 (2022).
10. C. Li, et al., "High-power III–V/Si integrated wavelength tunable laser for L-band applications," IEEE J. Quantum Electron. **59**, 1-6 (2023).